

# Comparison of SSFP and IR GRE Techniques for Measurement of Total Myocardial Mass-Influence of Applied Contrast Dosage and Implication for Relative Infarct Size Assessment

F. Grothues,<sup>1</sup> H. Boenigk,<sup>1</sup> A. Ghanem,<sup>1</sup> A. Schwerdtfeger,<sup>1</sup> D. Bartels,<sup>1</sup> S. Alpers,<sup>1</sup> C. Tempelmann,<sup>2</sup>  
and H. U. Klein<sup>1</sup>

Departments of Cardiology,<sup>1</sup> Neurology II,<sup>2</sup> Otto-von-Guericke-University, Magdeburg, Germany

## ABSTRACT

**Objective:** To compare total left ventricular mass assessment using steady state free precession (SSFP) and inversion recovery fast gradient echo (IR GRE) imaging and further to assess the influence of contrast dosage on mass by IR GRE and its implications on relative infarct size assessment with both methods. **Methods:** Forty-three patients with first documented myocardial infarction and single vessel disease underwent measurement of total myocardial mass using SSFP technique and an IR GRE sequence. As part of a Phase 2 multi-center dose ranging study for infarct identification patients received 1 of 4 possible dosages (0.05, 0.1, 0.2 or 0.3 mmol/kg body weight) of the contrast agent gadoversetamide (OptiMARK, Tyco Healthcare Mallinckrodt, St. Louis, MO, USA). **Results:** Left ventricular mass assessment using IR GRE resulted in a slightly greater detection of myocardial mass than from the SSFP images (160.1 and 156.4 g, respectively,  $p < 0.001$ ). The overall good correlation of both methods ( $R^2 = 0.97$  for the total study group,  $p < 0.001$ ) was further improved by using gadoversetamide at doses of 0.2 or 0.3 mmol/kg ( $R^2 = 0.99$ ,  $p < 0.001$ ), mainly as a result of a considerably higher blood-myocardial contrast-to-noise ratio (CNR) in the IR GRE images. Bland-Altman analysis in these subgroups showed very little scatter of the residuals over the mean ( $3.5 \pm 5.4$  g and  $1.3 \pm 6.9$  g respectively, 95% confidence interval). The observed differences in total mass calculation, while statistically significant, were not correlated with clinically relevant differences in estimation of relative infarct size. **Conclusion:** Total LV mass calculations using SSFP and IR GRE techniques are interchangeable when using appropriate contrast media, such as gadoversetamide. Late gadolinium enhancement results in good blood myocardial CNR. Hence, for relative infarct size assessment either method for calculation of total myocardial mass can be used.

Received 2 January 2006; accepted 4 June 2006.

**Keywords:** Late Gadolinium Enhancement, Cardiovascular Magnetic Resonance, Infarct Size, Myocardial Mass, Gadoversetamide.

We thank Prof. Dr. Hans-Joachim Heinze, director of the Department of Neurology II, Otto-von-Guericke-University Magdeburg, who generously provided the magnetic resonance scanning facility.

Correspondence to:

Dr. Frank Grothues

Department of Cardiology

Otto-von-Guericke-University

Leipziger Strasse 44

D-39120 Magdeburg

Germany

tel: +49-391-6713203; fax: +49-391-6713202

email: frank.grothues@medizin.uni-magdeburg.de

## INTRODUCTION

Since its first descriptions by Kim and Judd (1–3), the late gadolinium enhancement technique using inversion recovery fast gradient echo sequences (IR GRE) has emerged as an extremely valuable tool for the assessment of myocardial viability (4). It has been shown to accurately detect both Q-wave and non-Q-wave myocardial infarction (5) as well as to predict reversible myocardial dysfunction after myocardial infarction (6–8). Furthermore, late gadolinium enhancement proved to be more sensitive in detecting small infarcts in comparison to single photon emission computed tomography (SPECT) perfusion imaging (9, 10). Recent studies have further elucidated the potential of this technique in comparison to the current gold standard of positron emission tomography (PET) (11, 12). First prognostic data by use of late gadolinium enhancement have

been presented as well. In a multivariate analysis of a multicenter trial, Kaushal demonstrated that infarct size of more than 15% of left ventricular (LV) mass, as derived from cardiovascular magnetic resonance (CMR), had the highest predictive value for death (13).

Total LV mass itself can be measured in different ways. In the early days of CMR, black-blood techniques were used (14–16). Currently, cine bright blood techniques, such as gradient echo sequences (17–20) and especially steady state free precession sequences (SSFP) (21–24), are applied. Total infarct size usually is derived by planimetry of the late gadolinium enhanced area on a stack of short axis IR GRE images. For calculation of relative infarct size, the infarct mass is divided by the total LV mass.

Usually, the total LV mass calculation by SSFP is included in the analysis process of cine bright blood images for volumes and ejection fraction of the right and left ventricle. Using this SSFP derived mass reduces the need for another time consuming delineation of endocardial and epicardial borders in the IR GRE images. However, it has not yet been shown that mass calculations with SSFP and IR GRE are interchangeable. Thus, the use of SSFP derived mass may not accurately estimate relative infarct size, as absolute infarct size is measured in IR GRE images. The different imaging techniques with often different spatial resolutions and image acquisitions at different time points during the cardiac cycle may lead to differing results in total myocardial mass calculations. To our knowledge, a systematic comparison of mass calculation with these two methods and its implication for relative infarct size assessment has not yet been performed.

## METHODS

A total of 43 patients (37 male, mean age 53 years, mean LV ejection fraction of  $50\% \pm 7\%$  by CMR [range 35–67%]) underwent measurement of total myocardial mass with SSFP technique and an IR GRE sequence. Patients were included as part of a double-blinded, randomized, multi-center, Phase 2, dose ranging study to evaluate the safety and efficacy of gadoversetamide to identify the presence, location, and extent of acute (less than 16 days) or chronic (between 17 days and 6 months) myocardial infarction based on hyper-enhancement (25). All patients underwent coronary angiography with subsequent stent treatment of the target lesion. The myocardial infarct affected the LAD territory in 20 patients (47%), the RCA in 13 (30%) and the RCX in 10 patients (23%). Fifty-six percent of infarcts were predominantly transmural, and 44% were non-transmural. Image acquisition was performed at  $7 \pm 3$  days after the index infarct for the acute infarct study ( $n = 21$ ) and at  $78 \pm 44$  days after infarct for the chronic infarct study ( $n = 22$ ). The presented substudy reflects the analysis from a single site and is not related to the methods and analysis of the primary multi-center trial. Inclusion criteria comprised single vessel disease and documented first myocardial infarction. The study protocol was approved by the locally appointed ethics committee and all patients signed an informed consent before participation. The study complies with the Declaration of Helsinki.

## *Contrast agent and dosage scheme*

As part of a multicenter trial the paramagnetic contrast agent gadoversetamide (OptiMARK, Tyco Healthcare Mallinckrodt, St. Louis, MO, USA), a neutral (non-ionic), extracellular gadolinium-chelate was used. Patients were prospectively randomized to receive a weight adapted intravenous bolus of 4 possible concentrations of gadoversetamide (0.05, 0.1, 0.2, or 0.3 mmol/kg body weight). After contrast bolus application, the intravenous tube was flushed with 10 mL of isotonic saline.

## *Cardiovascular magnetic resonance scan*

All subjects were imaged on a Signa NVi 1.5 Tesla scanner (GE medical systems, Milwaukee, WI, USA), using a 4 element cardiac phased array coil and electrocardiographic triggering. All scans were performed by a single expert operator.

A diastolic 4 chamber view at end-expiration provided the reference image on which a stack of contiguous short-axis slices were positioned, with the first slice positioned at the atrioventricular ring, and the last slice covering the apex. Slice position was identical for both sequences especially to minimize for misregistration of the most basal slice.

## *SSFP sequence*

SSFP breath-hold cines with prospective ECG triggering were used for all slices with the following parameters: echo time (TE) 1.6 ms; repeat time (TR) 4.0 ms; slice thickness 6 mm; inter-slice gap 4 mm; rectangular field of view  $40 \times 30$  cm; read matrix 224; phase matrix 224; calculated frames 40; flip angle  $45^\circ$ ; views per segment 10–24 (depending on heart rate). A total of 8 to 12 short-axis segments were needed to encompass the entire LV. Mean acquisition time for each breath-hold was about 12 seconds.

## *IR GRE sequence*

For late gadolinium enhancement a segmented IR GRE breath-hold sequence was used with the following parameters: echo time (TE) 3.2 ms; repeat time (TR) 7.3 ms; slice thickness 6 mm; inter-slice gap 4 mm; rectangular field of view  $36 \times 27$  cm; read matrix 256; phase matrix 192; flip angle  $20^\circ$ ; views per segment 18–34 (depending on heart rate). Images were acquired with every, or every other heartbeat. Mean acquisition time for each breath-hold was about 14 seconds. To ensure direct comparison, short-axis slice orientation was identical with the SSFP acquisition. Inversion times varied between 160 and 380 ms, mainly depending on contrast dosage applied. Image acquisition for late gadolinium enhancement started 10 minutes after application of gadoversetamide.

## *Image analysis*

CMR image analysis was performed by a single experienced investigator (the same person who operated the scanner) using commercial software (Mass analysis software, MEDIS, Leiden, the Netherlands). Manual tracing of left ventricular endocardial

**Table 1.** Total left ventricular mass (g) assessed with both techniques for the total study group (except 0.05 mmol/kg subgroup) and divided up by contrast dosage

Left ventricular mass (g)	0.1 (n = 11)	0.2 (n = 11)	0.3 (n = 11)	Total (n = 33)
IR GRE	168.9 ± 31.0	151.8 ± 32.5	159.6 ± 32.8	160.1 ± 31.9
SSFP	162.5 ± 32.7	148.4 ± 31.7	158.4 ± 31.7	156.4 ± 31.6
Mass Difference (IR GRE – SSFP) in g	6.5 ± 7.5	3.5 ± 2.7	1.3 ± 3.5	3.7 ± 5.3
Mass Difference (IR GRE – SSFP) in % of mean mass	4.2 ± 4.8	2.3 ± 2.0	0.7 ± 2.3	2.4 ± 3.5
p value (paired t-test, 2-tailed)	0.018	0.002	0.251	< 0.001

and epicardial borders of contiguous short-axis slices at end-diastole (first cine phase of the R-wave triggered acquisition) allowed calculation of left myocardial mass with SSFP images. On late gadolinium enhancement images (IR GRE), left endocardial and epicardial contours were also manually traced for myocardial mass calculation. Papillary muscles were included in the mass and excluded from the volume. Absolute infarct size in grams was measured by manual planimetry of the late gadolinium enhanced regions in the IR GRE images. Values for relative infarct size were derived by dividing absolute infarct size by total left ventricular mass (separately for each imaging technique). To avoid a memory effect the myocardial mass by SSFP and IR GRE was analyzed a minimum of 2 weeks apart from each other, with the investigator blinded to the subject's name and the previous results.

On a representative short-axis IR GRE image of each patient, regions of interest (ROI) were drawn in the myocardium and blood pool for signal intensity measurements as well as at the edge of each CMR image outside the chest for measurement of background noise. The area of the ROI chosen for each series was the maximum permissible without causing contamination from other adjacent tissues: 3.4 cm<sup>2</sup> for blood (range 1.2–3.5 cm<sup>2</sup>); 0.6 cm<sup>2</sup> for myocardium (range 0.3–1.0 cm<sup>2</sup>); and 3.5 cm<sup>2</sup> consistently for background noise. The blood-myocardial contrast-to-noise ratio (CNR<sub>bm</sub>) was calculated with the following equation:  $CNR_{bm} = (SI_b - SI_m)/SD_n$  where  $SI_b$  is the signal intensity of blood,  $SI_m$  is the signal intensity of myocardium, and  $SD_n$  is the standard deviation of background noise (26).

### Statistical analysis

Data are presented as mean and standard deviation (SD). Statistical significance of group means was assessed with paired or unpaired Student t-test (two-tailed). Linear regression analysis was performed to determine the strength of correlation be-

tween left myocardial mass obtained by SSFP and IR GRE. A Bland-Altman analysis was used to determine the 95% limits of agreement between the 2 methods. Scatterplots and correlation coefficients (reported as R<sup>2</sup> and calculated using a Pearson test) are only a measure of the linearity of the relation between 2 variables and do not indicate the strength of agreement between techniques, for which Bland-Altman plots are more appropriate (27). For all statistical analyses, a p value smaller than 0.05 was considered statistically significant.

## RESULTS

The 0.05 mmol/kg dose resulted in such a low contrast of the LV blood pool that the endocardial border in IR GRE images was undiscernible in 8 of 10 patients receiving this dose. Therefore, the 0.05 subgroup was excluded from the mass comparison. In the remainder 33 patients left ventricular mass assessment with IR GRE resulted in a slightly greater myocardial mass than assessment with SSFP images (160.1 and 156.4 g, respectively,  $p < 0.001$ ), which was statistically significant in all subgroups except the 0.3 group (Table 1). The absolute mass difference varied between 1.3 g for the 0.3 dosage and 6.5 g for the 0.1 dosage group with percentage differences between 0.7 and 4.2%.

Linear regression analysis showed a good correlation between both imaging techniques (R<sup>2</sup> = 0.97 for the total study group,  $p < 0.001$ ). Divided by subgroups, the correlation was strongest with the 0.2 and 0.3 dosage groups (R<sup>2</sup> = 0.99 and  $p < 0.001$  for both) and weakest with the 0.1 dosage group (R<sup>2</sup> = 0.95,  $p < 0.001$ ). The Bland-Altman plots (Fig. 1) display the differences between the mean myocardial mass assessed by both imaging techniques. As the contrast dosage increases, the residuals over the mean became smaller.

The effect of total myocardial mass differences on the calculation of relative infarct size is shown in Table 2. For the total

**Table 2.** Relative infarct size (% of total left ventricular mass) calculated by both techniques divided up by contrast dosage and for the total study group (except 0.05 mmol/kg subgroup)

Relative infarct size (%)	0.1 (n = 11)	0.2 (n = 11)	0.3 (n = 11)	Total (n = 33)
SSFP	16.3 ± 5.5	18.6 ± 7.8	14.7 ± 4.8	16.5 ± 6.2
IR GRE	15.6 ± 5.3	18.2 ± 7.7	14.5 ± 4.6	16.1 ± 6.0
Difference in relative infarct size	0.7 ± 0.9	0.4 ± 0.4	0.1 ± 0.4	0.4 ± 0.6
p value (paired t-test, 2-tailed)	<b>0.031</b>	<b>0.006</b>	0.248	<b>0.001</b>

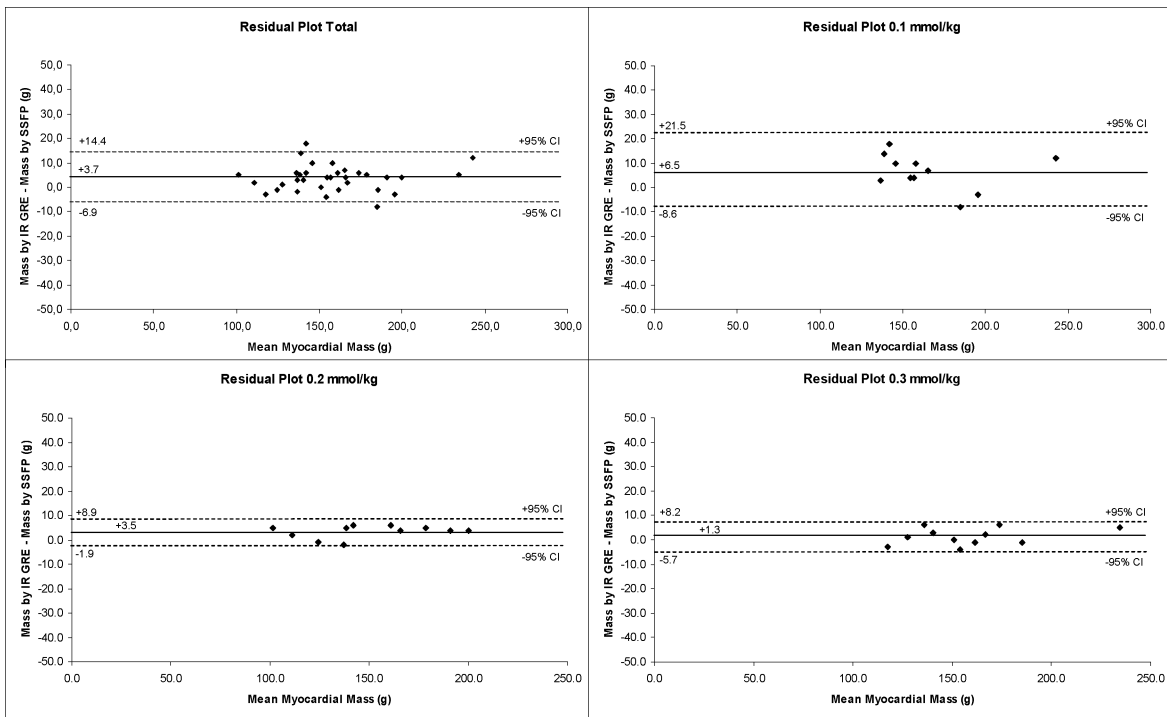


**Figure 1.** Residual plots (Bland Altman analysis) displaying 95% limits of agreement (dashed lines) between IR GRE and SSFP for left ventricular mass assessment for the total study group (upper left) and all analysed subgroups. Mean difference between measurements (solid line) is also shown.

study group, relative infarct size was smaller when IR GRE mass measurement was used for calculation ( $p = 0.001$ ). Within the subgroups, the difference in relative infarct sizes was not significant in the group with the highest (0.3) contrast dosage.

The results of the  $CNR_{bm}$  measurements are shown in Figure 2. A marked rise in  $CNR_{bm}$  is observed with the two highest dosage groups (0.2 and 0.3 mmol/kg). Figure 3 displays the effect of the contrast-to-noise ratio in IR GRE images on the mass differences between imaging techniques. With increasing contrast-to-noise ratio, a slight decrease in residuals can be observed.

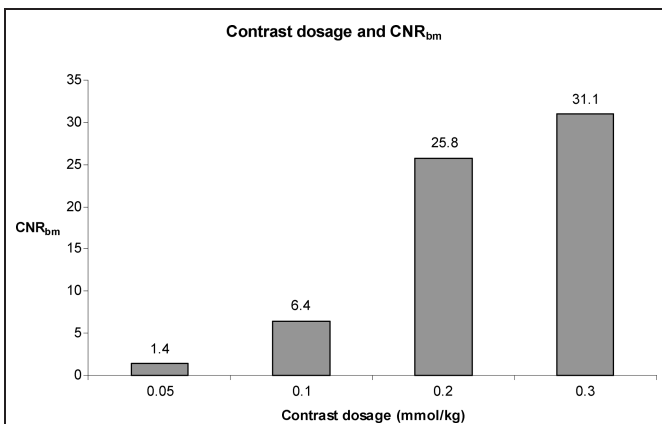


**Figure 2.** Blood-myocardial contrast-to-noise ratios ( $CNR_{bm}$ ) in relation to the contrast dosages under investigation.

erved. This is not as obvious when looking at the residuals of relative infarct size assessment (Fig. 4).

Chronicity of the infarct did not affect the difference of mass measurements in our study ( $p = 0.54$ , unpaired Students t-test). Mean difference was  $3.1 \pm 5.9$  g for the acute and  $4.3 \pm 4.9$  g for the chronic infarct group (Bland-Altman limits of agreement  $-8.7$  to  $14.9$  g and  $-5.5$  to  $14.1$  g, respectively).

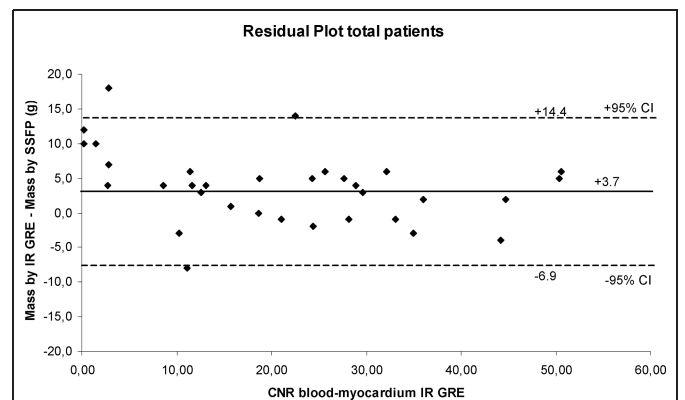


**Figure 3.** Residual plot (Bland Altman analysis) displaying 95% limits of agreement (dashed lines) for left ventricular mass assessment between IR GRE and SSFP in relation to the blood-myocardial contrast-to-noise ratio ( $CNR_{bm}$ ) on IR GRE images. The solid line displays the mean difference.

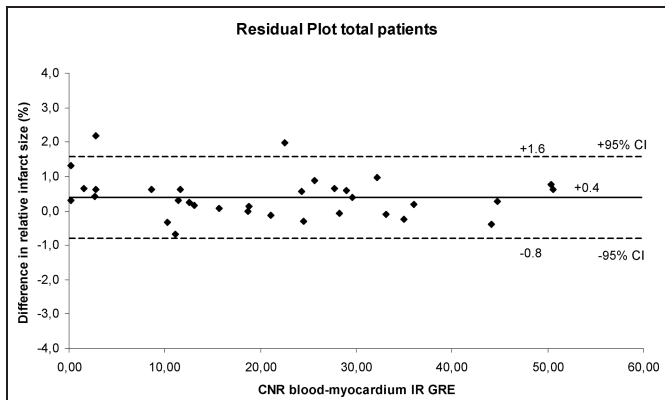


**Figure 4.** Residual plot with 95% limits of agreement for relative infarct size calculation between IR GRE and SSFP in relation to the blood-myocardial contrast to noise ratio ( $CNR_{bm}$ ) on IR GRE images. The mean difference between measurements is shown as a solid line.

## DISCUSSION

Bright blood cine acquisitions with GRE or SSFP techniques currently represent an integral part of a comprehensive cardiac magnetic resonance exam. Measurements (eg, left and right end-diastolic and end-systolic volumes, ejection fraction, total LV mass) using these techniques are calculated and have been proven to be accurate and reproducible (19, 20, 28, 29). With ischemic heart disease, IR GRE sequences (commonly described as late gadolinium enhancement technique) for infarct imaging have considerably contributed to the diagnostic spectrum of cardiovascular magnetic resonance (2, 4). Single-center studies have shown a sensitivity for infarct detection, which appears to be superior to SPECT (9,10) and to the current gold standard of PET (11, 12). Absolute and, perhaps more importantly, relative infarct size assessment by CMR can serve as a surrogate parameter in studies evaluating treatment strategies for patients with myocardial infarction (30, 31). Moreover, researchers from 5 centers recently could demonstrate the predictive value of CMR measured infarct size in 100 patients (13). Among other risk factors (eg, congestive heart failure (CHF) symptoms, ejection fraction (EF), severity of coronary artery disease (CAD)) only a relative infarct size of more than 15% of LV mass and reduced LVEF were independent predictors of outcome with CMR-derived infarct size of more than 15% showing the highest predictive value for death. In another study, Bello demonstrated that total infarct mass identified patients with a tendency for monomorphic ventricular arrhythmias better than LV ejection fraction (32).

For relative infarct size calculations, total LV mass by either SSFP (30, 33) or IR GRE (11, 34–38) techniques may be used. However, the ability to interchange mass calculations with SSFP and IR GRE has not yet been demonstrated. Because absolute infarct size is determined in IR GRE images, the use of SSFP-derived total mass may not accurately reflect relative infarct size.

The present study is the first to systematically investigate the differences in mass assessment with both techniques and to as-

sess the influence of contrast dosage in IR GRE images. Overall, we found great similarity between the 2 techniques in determining left myocardial mass with in general lower values with the SSFP sequence in comparison to the IR GRE technique. This finding is in accord with the results found by Klein in 31 patients (11). Klein also reported a slightly higher mass derived from late gadolinium enhanced IR GRE images than with SSFP technique (135 and 132 g, respectively) with a good correlation between methods ( $R^2 = 0.88$ , slope 0.84,  $p < 0.0001$ ). To our knowledge, these very limited data by Klein represent the only analysis in the literature with regard to left ventricular mass comparisons between IR GRE and SSFP. Previous studies comparing SSFP and cine GRE techniques for mass calculation also resulted in lower mass values with the SSFP sequence (22, 23).

As can be seen from Figure 5, the delineation of the myocardial blood-pool border is barely discernable from the 0.05 mmol/kg dose and mass analysis cannot be accurately performed at that dose. Therefore, we excluded this dosage group from further mass analysis. The mean differences within the rest of our total study group were small (3.7 g, 2.4%); the largest mean difference (6.5 g, 4.2%) occurred in the subgroup with the 0.1 mmol/kg dosage. With increasing contrast dosage the difference between both methods diminished (Table 1) and the correlation in the linear regression analysis increased. Scatterplots and correlation coefficients are a measure of the linearity of the relation between 2 variables but do not indicate the strength of agreement between techniques, in which case Bland-Altman plots are more appropriate (27). Bland-Altman plots showed a decrease in the residuals over the mean mass of both techniques with increasing contrast dosage (Fig. 1). Subgroup analysis of total mass calculation reflects the importance of an appropriate amount of contrast not only for good delineation of the infarct zone, but also for a better border definition of blood pool and myocardium. Figure 5 shows representative IR GRE images of 4 patients with the 4 different contrast dosages used in this trial. Apart from a better definition of infarcted tissue, the higher contrast dosages provide a better enhancement of the blood pool. As a consequence, the delineation of the myocardial-blood pool border is hardly possible at the lowest contrast dosage (Fig. 5, upper left), whereas it is much easier to detect at the higher contrast dosages of 0.2 and 0.3 mmol/kg (Fig. 5, bottom row). This visual impression is confirmed by an increase of blood-myocardial CNR with increasing contrast dosage (Fig. 2). Consequently, the Bland-Altman plots demonstrated a decrease of differences in total mass between techniques (Fig. 3) with increasing  $CNR_{bm}$ .

To put the small differences observed between IR GRE and SSFP imaging into perspective, we compared them to the differences of mass calculation with SSFP at end-diastole and end-systole. The means, of both measurements were not significantly different ( $p = 0.5$ ) and the mean difference between mass at end-diastole and at end-systole was  $-0.7 \pm 5.2$  g with Bland-Altman limits of agreement calculated as  $-11.1$  to 9.7 g. Compared to the difference observed between IR GRE and SSFP mass calculation of this mean difference proved to be significantly lower ( $p < 0.001$ ).

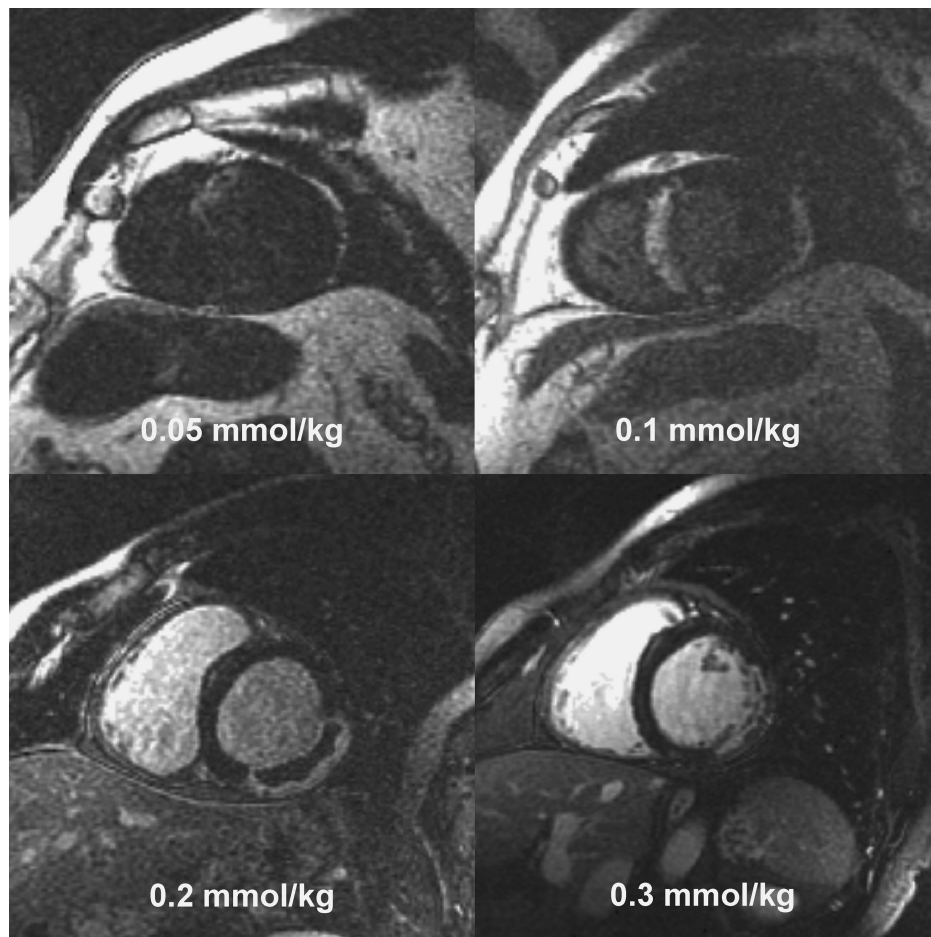


**Figure 5.** Examples of IR GRE images for infarct detection in four patients obtained with the four different contrast dosages under investigation (0.05 mmol/kg top left, 0.1 mmol/kg top right, 0.2 mmol/kg bottom left and 0.3 mmol/kg bottom right). Blood-myocardial contrast is evidently best with the two highest contrast dosages (bottom row). Interestingly, a huge zone of microvascular obstruction without late gadolinium enhancement surrounded by enhanced infarcted tissue is present in the posterolateral infarct (bottom left). A smaller area of microvascular obstruction can be seen in the infarct core of the right bottom image.

Independent of the amount of contrast applied, a common problem of myocardial mass assessment with the IR GRE technique is the poor border definition of signal nulled myocardium and lung tissue in the lateral and posterolateral regions of the left ventricle.

It should be noted that because the absolute differences in total myocardial mass were small (but statistically significant except for the 0.3 group), they did not lead to clinically relevant differences in relative infarct size. The difference was significant only for the 0.1 and 0.2 dosage groups and for the total study population. However, a mean difference in relative infarct size of 0.4% as for our total study group is clinically negligible. Hence, in our opinion, either SSFP or IR GRE can be used for mass calculation, provided an appropriate contrast dosage has been chosen for the IR GRE acquisition. The decision on which method to use can, therefore, be tailored upon the other questions to be answered during the CMR exam. If a left ventricular function study is part of the cardiac exam, SSFP images can be used for total left ventricular mass assessment and relative

infarct size calculation without the need for a redo of total mass calculation from IR GRE images.

### *Study limitations*

Since the inclusion criteria comprised only patients with first myocardial infarct and single vessel disease, our study group on average represents patients with relatively small infarcts and only mildly reduced ejection fraction. Although some of our patients in the chronic infarct group presented with large infarcts, a mean follow-up time of on average 78 days might be too early for a complete ventricular remodeling. Therefore, it remains unclear whether these findings are also applicable to patients with multivessel disease, lower LVEF and associated reverse remodeling (e.g., extensive wall thinning and large apical aneurysms).

Although the total study group represents a sufficient number of patients, separated for each dosage patient numbers were relatively small (11, 10 patients respectively). The same applies to the relatively narrow range of masses with the bulk of patients

lying between 100–200 grams of total left ventricular myocardial mass.

SSFP imaging in comparison to standard gradient echo techniques in several studies in humans (22, 23) has shown to result in lower values for left ventricular mass and greater values for ventricular volumes. The study protocol did not contain a standard gradient echo sequence for mass assessment, since, due to acquisition speed and good blood-myocardial contrast, SSFP imaging today has evolved as the standard cine imaging sequence on most scanners. We did not aim to find out and, therefore, cannot conclusively rate whether mainly the use of the SSFP sequence or inherent properties of the IR GRE technique led to the small differences observed.

Slice position of the short axis views was identical for both sequences. Although this approach somewhat eased the definition of the most basal slice with the IR GRE sequence, mass calculation with SSFP and IR GRE techniques happens at different time points of the cardiac cycle. Therefore, measurement errors due to poor definition of the basal slice in the single image of a IR GRE sequence cannot be fully eliminated.

Image acquisition with the IR GRE sequence was performed every heartbeat (majority of patients) or every other heartbeat. Due to the small numbers, we were not able to detect any reliable differences between these two approaches. Theoretically, with the technique of scanning every second heartbeat, contrast in the infarcted areas may slightly improve with subsequent effect on the estimation of total LV mass.

## CONCLUSION

Total myocardial mass calculation with IR GRE and SSFP techniques show a good overall correlation with excellent results when an appropriate contrast dosage is used. With the prerequisite of a good blood-myocardial CNR, SSFP and IR GRE techniques are interchangeable. Even with integration of the lower contrast dosage of 0.1 mmol/kg, the observed differences in total mass between techniques do not translate into clinical relevant differences of relative infarct size calculation.

## REFERENCES

1. Kim RJ, Fieno DS, Parrish TB, Harris K, Chen EL, Simonetti O, et al. Relationship of MRI delayed contrast enhancement to irreversible injury, infarct age, and contractile function. *Circulation* 1999;100:1992–2002.
2. Simonetti OP, Kim RJ, Fieno DS, Hillenbrand HB, Wu E, Bundy JM, et al. An improved MR imaging technique for the visualization of myocardial infarction. *Radiology* 2001;218:215–23.
3. Fieno DS, Kim RJ, Chen EL, Lomasney JW, Klocke FJ, Judd RM. Contrast-enhanced magnetic resonance imaging of myocardium at risk: distinction between reversible and irreversible injury throughout infarct healing. *J Am Coll Cardiol* 2000;36:1985–91.
4. Pennell DJ, Sechtem UP, Higgins CB, Manning WJ, Pohost GM, Rademakers FE, et al. Clinical indications for cardiovascular magnetic resonance (CMR): Consensus Panel report. *Eur Heart J* 2004;25:1940–65.
5. Wu E, Judd RM, Vargas JD, Klocke FJ, Bonow RO, Kim RJ. Visualisation of presence, location, and transmural extent of healed Q-wave and non-Q-wave myocardial infarction. *Lancet* 2001;357:21–8.
6. Kim RJ, Wu E, Rafael A, Chen EL, Parker MA, Simonetti O, et al. The use of contrast-enhanced magnetic resonance imaging to identify reversible myocardial dysfunction. *N Engl J Med* 2000;343:1445–53.
7. Gerber BL, Garot J, Bluemke DA, Wu KC, Lima JA. Accuracy of contrast-enhanced magnetic resonance imaging in predicting improvement of regional myocardial function in patients after acute myocardial infarction. *Circulation* 2002;106:1083–9.
8. Ramani K, Judd RM, Holly TA, Parrish TB, Rigolin VH, Parker MA, et al. Contrast magnetic resonance imaging in the assessment of myocardial viability in patients with stable coronary artery disease and left ventricular dysfunction. *Circulation* 1998;98:2687–94.
9. Wagner A, Mahrholdt H, Holly TA, Elliott MD, Regenfus M, Parker M, et al. Contrast-enhanced MRI and routine single photon emission computed tomography (SPECT) perfusion imaging for detection of subendocardial myocardial infarcts: an imaging study. *Lancet* 2003;361:374–9.
10. Kitagawa K, Sakuma H, Hirano T, Okamoto S, Makino K, Takeda K. Acute myocardial infarction: myocardial viability assessment in patients early thereafter: comparison of contrast-enhanced MR imaging with resting (201)TI SPECT. *Radiology* 2003;226:138–44.
11. Klein C, Nekolla SG, Bengel FM, Momose M, Sammer A, Haas F, et al. Assessment of myocardial viability with contrast-enhanced magnetic resonance imaging: comparison with positron emission tomography. *Circulation* 2002;105:162–7.
12. Kuhl HP, Beek AM, van der Weerd AP, Hofman MB, Visser CA, Lammertsma AA, et al. Myocardial viability in chronic ischemic heart disease: comparison of contrast-enhanced magnetic resonance imaging with (18)F-fluorodeoxyglucose positron emission tomography. *J Am Coll Cardiol* 2003;41:1341–8.
13. Kaushal R, Fieno D, Radin M, Shaoulian E, Narula J, Goldberger J, et al. Infarct size is an independent predictor of mortality in patients with coronary artery disease [abstract]. *J Cardiovasc Magn Reson* 2005;7:39A–40A.
14. Caputo GR, Suzuki J, Kondo C, Cho H, Quaipe RA, Higgins CB, et al. Determination of left ventricular volume and mass with use of biphasic spin-echo MR imaging: comparison with cine MR. *Radiology* 1990;177:773–7.
15. Florentine MS, Grosskreutz CL, Chang W, Hartnett JA, Dunn VD, Erhardt JC, et al. Measurement of left ventricular mass in vivo using gated nuclear magnetic resonance imaging. *J Am Coll Cardiol* 1986;8:107–12.
16. Forbat SM, Karwatowski SP, Gatehouse PD, Firmin DN, Longmore DB, Underwood SR. Rapid measurement of left ventricular mass by spin echo magnetic resonance imaging [technical note]. *Br J Radiol* 1994;67:86–90.
17. Matheijssen NA, Baur LH, Reiber JH, van der Velde EA, van Dijkman PR, van der Geest RJ, et al. Assessment of left ventricular volume and mass by cine magnetic resonance imaging in patients with anterior myocardial infarction: intra-observer and inter-observer variability on contour detection. *Int J Card Imaging* 1996;12:11–9.
18. Sakuma H, Fujita N, Foo TK, Caputo GR, Nelson SJ, Hartiala J, et al. Evaluation of left ventricular volume and mass with breath-hold cine MR imaging. *Radiology* 1993;188:377–80.
19. Grothues F, Smith GC, Moon JC, Bellenger NG, Collins P, Klein HU, et al. Comparison of interstudy reproducibility of Cardiovascular magnetic resonance with two-dimensional echocardiography in normal subjects and in patients with heart failure or left ventricular hypertrophy. *Am J Cardiol* 2002;90:29–34.
20. Bellenger NG, Davies LC, Francis JM, Coats AJ, Pennell DJ. Reduction in sample size for studies of remodeling in heart failure by the use of cardiovascular magnetic resonance. *J Cardiovasc Magn Reson* 2000;2:271–8.

21. Fuchs F, Laub G, Othomo K. TrueFISP—technical considerations and cardiovascular applications. *Eur J Radiol* 2003;46:28–32.
22. Moon JC, Lorenz CH, Francis JM, Smith GC, Pennell DJ. Breath-hold FLASH and FISP cardiovascular MR imaging: left ventricular volume differences and reproducibility. *Radiology*. 2002;223:789–97.
23. Plein S, Bloomer TN, Ridgway JP, Jones TR, Bainbridge GJ, Sivananthan MU. Steady-state free precession magnetic resonance imaging of the heart: comparison with segmented k-space gradient-echo imaging. *J Magn Reson Imaging*. 2001;14:230–6.
24. Barkhausen J, Ruehm SG, Goyen M, Buck T, Laub G, Debatin JF. MR evaluation of ventricular function: true fast imaging with steady-state free precession versus fast low-angle shot cine MR imaging: feasibility study. *Radiology*. 2001;219:264–9.
25. Kim RJ, Albert TSE, Wible JH Jr, Elliott MD, Allen JC Jr, Lee JC, Napoli A, Judd RM. Efficacy of gadoversetamide-enhanced MRI for the diagnosis and assessment of myocardial infarction: an international, multicenter, double-masked, randomized, phase 2 trial [abstract]. *J Am Coll Cardiol* 2005;45:287A–8A.
26. Kaufman L, Kramer DM, Crooks LE, Ortendahl DA. Measuring signal-to-noise ratios in MR imaging. *Radiology* 1989;173:265–7.
27. Bland JM, Altman DG. Statistical methods for assessing agreement between two methods of clinical measurement. *Lancet* 1986;1:307–10.
28. McDonald KM, Parrish T, Wennberg P, Stillman AE, Francis GS, Cohn JN, et al. Rapid, accurate and simultaneous noninvasive assessment of right and left ventricular mass with nuclear magnetic resonance imaging using the snapshot gradient method. *J Am Coll Cardiol* 1992;19:1601–7.
29. Shapiro EP, Rogers WJ, Beyar R, Soulen RL, Zerhouni EA, Lima JA, et al. Determination of left ventricular mass by magnetic resonance imaging in hearts deformed by acute infarction. *Circulation* 1989;79:706–11.
30. Gick M, Jander N, Bestehorn HP, Kienzle RP, Ferenc M, Werner K, et al. Randomized evaluation of the effects of filter-based distal protection on myocardial perfusion and infarct size after primary percutaneous catheter intervention in myocardial infarction with and without ST-segment elevation. *Circulation* 2005;112:1462–9.
31. Thiele H, Engelmann L, Elsner K, Kappl MJ, Storch WH, Rahimi K, et al. Comparison of pre-hospital combination-fibrinolysis plus conventional care with pre-hospital combination-fibrinolysis plus facilitated percutaneous coronary intervention in acute myocardial infarction. *Eur Heart J* 2005;26:1956–63.
32. Bello D, Fieno DS, Kim RJ, Pereles FS, Passman R, Song G, et al. Infarct morphology identifies patients with substrate for sustained ventricular tachycardia. *J Am Coll Cardiol* 2005;45:1104–8.
33. van Dockum WG, ten Cate FJ, ten Berg JM, Beek AM, Twisk JW, Vos J, et al. Myocardial infarction after percutaneous transluminal septal myocardial ablation in hypertrophic obstructive cardiomyopathy: evaluation by contrast-enhanced magnetic resonance imaging. *J Am Coll Cardiol* 2004;43:27–34.
34. Slomka PJ, Fieno D, Thomson L, Friedman JD, Hayes SW, Germano G, et al. Automatic detection and size quantification of infarcts by myocardial perfusion SPECT: clinical validation by delayed-enhancement MRI. *J Nucl Med* 2005;46:728–35.
35. Haase J, Bayar R, Hackenbroch M, Storger H, Hofmann M, Schwarz CE, et al. Relationship between size of myocardial infarctions assessed by delayed contrast-enhanced MRI after primary PCI, biochemical markers, and time to intervention. *J Interv Cardiol* 2004;17:367–73.
36. Petersen SE, Mohrs OK, Horstick G, Oberholzer K, Abegunewardene N, Ruetzel K, et al. Influence of contrast agent dose and image acquisition timing on the quantitative determination of non-viable myocardial tissue using delayed contrast-enhanced magnetic resonance imaging. *J Cardiovasc Magn Reson* 2004;6:541–8.
37. Ingkanisorn WP, Rhoads KL, Aletras AH, Kellman P, Arai AE. Gadolinium delayed enhancement cardiovascular magnetic resonance correlates with clinical measures of myocardial infarction. *J Am Coll Cardiol* 2004;43:2253–9.
38. Azevedo Filho CF, Hadlich M, Petriz JL, Mendonca LA, Moll Filho JN, Rochitte CE. Quantification of left ventricular infarcted mass on cardiac magnetic resonance imaging: comparison between planimetry and the semiquantitative visual scoring method. *Arq Bras Cardiol* 2004;83:118–24.